Effect of endothelin receptor antagonists on ventricular susceptibility in postinfarcted rats

Tsung-Ming Lee, Chien-Chang Chen, Mei-Shu Lin and Nen-Chung Chang

Am J Physiol Heart Circ Physiol 294:H1871-H1879, 2008. First published 15 February 2008; doi:10.1152/ajpheart.01129.2007

Am J Physiol Heart Circ Physiol 294: H1871–H1879, 2008.
First published February 15, 2008; doi:10.1152/ajpheart.01129.2007.

Effect of endothelin receptor antagonists on ventricular susceptibility in postinfarcted rats

Tsung-Ming Lee,[1] Chien-Chang Chen,[2] Mei-Shu Lin,[3] and Nen-Chung Chang[4]

[1]*Cardiology Section, Department of Medicine, Taipei Medical University and Chi-Mei Medical Center;* [2]*Cardiology Section, Department of Surgery, Chi-Mei Medical Center;* [3]*Department of Pharmacy, National Taiwan University and Hospital;* [4]*Cardiology Section, Department of Medicine, Taipei Medical University and Hospital, Taipei, Taiwan*

Submitted 29 September 2007; accepted in final form 11 February 2008

Lee TM, Chen CC, Lin MS, Chang NC. Effect of endothelin receptor antagonists on ventricular susceptibility in postinfarcted rats. *Am J Physiol Heart Circ Physiol* 294: H1871–H1879, 2008. First published February 15, 2008; doi:10.1152/ajpheart.01129.2007.—This study investigated whether selective endothelin (ET) type A (ET_A) or nonselective ET_A/ET_B receptor blockade exerted antiarrhythmic effects through attenuated sympathetic reinnervation after infarction. Twenty-four hours after ligation of the left anterior descending artery, male Wistar rats received either vehicle, ABT-627 (selective ET_A receptor antagonist), bosentan (nonselective ET_A/ET_B receptor antagonist), or hydralazine for 4 wk. The measurement of myocardial ET-1 levels at the remote zone revealed a significant increase in vehicle-treated infarcted rats compared with sham-operated rats, consistent with increased activities of ET-1 after infarction. Sympathetic nerve function changes assessed by the norepinephrine content of myocardium and the dialysate and plasma dihydroxyphenylglycol levels were parallel to ET-1 levels. Immunohistochemical analysis for tyrosine hydroxylase, growth-associated protein 43, and neurofilament also confirmed the change of nerve function. This was accompanied with a significant upregulation of nerve growth factor protein expression and mRNA in the vehicle-treated infarcted rats, which reduced after the administration of either ET_A or ET_A/ET_B blockade to a similar extent. The beneficial effects of ET receptor antagonists on sympathetic nerve function and structures were dissociated from their blood pressure-lowering effect because ET receptor antagonists and hydralazine reduced arterial pressure similarly. Arrhythmic severity during programmed stimulation in ET receptor antagonists-treated rats was significantly lower than that in vehicle-treated infarcted rats. Our data indicate that the ET system, especially via ET_A receptors, plays an important role in attenuating sympathetic reinnervation after infarction. Independent of their hemodynamic effects, a chronic use of either ET_A or ET_A/ET_B antagonists may modify the arrhythmogenic response to programmed electrical stimulation.

myocardial infarction; nerve growth factor; rats; sympathetic reinnervation

WE HAVE PREVIOUSLY DEMONSTRATED that pravastatin improves ventricular remodeling and arrhythmic susceptibility through attenuated endothelin (ET)-1 expression after infarction (21). The ET system is activated in various pathophysiological states including postinfarction ventricular remodeling (31). ET-1 exerts biological activities through stimulation of the ET types A (ET_A) and B (ET_B) receptors (31). ET_A receptor antagonists are known to improve the prognosis of heart failure by preventing cardiac remodeling and ventricular dysfunction (32). ET_A receptor antagonists also have an antiarrhythmic effect in pathological hearts, although the mechanism remains unclear (24). Neural remodeling in sympathetic nerve sprouting results in ventricular tachyarrhythmia in diseased human hearts and in animal models (6, 7). ET-1 has been shown to upregulate nerve growth factor (NGF) mRNA and protein expression through an ET_A receptor pathway during the development of cardiac sympathetic innervation (17). NGF is a prototypic member of the neurotrophin family, members of which are critical for the differentiation, survival, and synaptic activity of the peripheral sympathetic and sensory nervous systems (23, 33). Levels of NGF expression within innervated tissues roughly correspond to innervation density (16). The deletion of a single copy of the *NGF* gene results in a 50% reduction in sympathetic neurons (5), whereas the overexpression of NGF in the heart results in cardiac hyperinnervation (14). These results demonstrated the importance of NGF in the regulation of sympathetic innervation.

Increased sympathetic nerve density after myocardial injury has been shown to be responsible for the occurrence of lethal arrhythmias and sudden cardiac death in humans (7). The observation was further supported by the finding of Du et al. (10), showing that the severity of pacing-induced ventricular arrhythmias can be attenuated by administering β-blockers in a dose-dependent manner in infarcted rat hearts. This provided direct evidence for a cause and effect relation between activation of sympathetic nerves and onset of ventricular arrhythmias in infarcted rat hearts. During the chronic stage of myocardial infarction, a regional increase of sympathetic nerves was commonly observed at the remote zone (34). Increased sympathetic nerve activity plays an important role in the generation of ventricular arrhythmia and sudden cardiac death (7). Thus nerve spouting has been shown to be an important contributing factor for the occurrence of ventricular arrhythmias and sudden cardiac death in healing or healed stages of infarction in animals (6, 19) and humans (4). We assessed *1*) whether chronic administration of ET receptor antagonists (ERAs) can result in attenuated heart reinnervation after infarction and *2*) which ET receptor subtypes underlie the ET-1-dependent nerve sprouting. Because regional sympathetic innervation reflected electrophysiological differences, we explored the downstream functional significance of attenuated heart reinnervation by ventricular pacing in a rat myocardial infarction model.

METHODS

Animals. Male normotensive Wistar rats (300–350 g) were subjected to ligation of the anterior descending artery as previously

Address for reprint requests and other correspondence: N.-C. Chang, Cardiology Sect., Dept. of Medicine, Taipei Medical Univ., 252, Wu-Hsing St., Taipei, Taiwan (e-mail: ncchang@tmu.edu.tw).

The costs of publication of this article were defrayed in part by the payment of page charges. The article must therefore be hereby marked "*advertisement*" in accordance with 18 U.S.C. Section 1734 solely to indicate this fact.

described (21), resulting in infarction of the left ventricular (LV) free wall. Rats were randomly assigned into four groups so as to have approximately the same number of survivors in each group (Table 1): *1*) vehicle group; *2*) 5 mg·kg^{-1}·day^{-1} 2*R*-(4-methoxyphenyl)-4*S*-(1,3-benzodioxol-5-yl)-1-[*N*,*N*-di(*n*-butyl)aminocarbonyl-methyl]-pyrrolidine-3*R*-carboxylic acid (ABT-627; Abbott Park, IL), a selective ET_A receptor antagonist; *3*) bosentan (100 mg·kg^{-1}·day^{-1}; Actelion Pharmaceuticals, Allschwil, Switzerland), a nonselective ET_A/ET_B receptor antagonist; and *4*) hydralazine (10 mg·kg^{-1}·day^{-1}). The dose of ABT-627 was chosen because it blocked the ET_A-mediated sustained vasoconstriction to ET-1 without affecting ET_B-mediated transient vasodilatation (1). The dose of bosentan (100 mg/kg) was given according to previous studies (28). Because ERAs have a blood pressure-lowering effect, hydralazine was used to exclude the confounding effect of blood pressure lowering on the sprouting of new cardiac nerves. Sham-operated rats underwent the same surgical procedures except for ligation.

The drugs were started 24 h after infarction, since drugs can exert maximum benefits during this time window (35). The study duration was designed to be 4 wk because the majority of the myocardial remodeling process in the rat (70–80%) is complete within 3 wk (3). The drugs were administered by daily oral gavage. In each treated group, drugs were withdrawn about 24 h before the end of the experiments to eliminate their pharmacological actions.

Sympathetic reinnervation has been shown to be present 4 days after injury (13). To differentiate the attenuated sympathetic reinnervation of ET receptor blockers from either inhibiting sympathetic reinnervation at the late stage of infarction or enhancing nerve degeneration at the early stage of infarction, we performed another experiment that ended at *postinfarction day 3* when sympathetic reinnervation did not occur. Twenty supplementary infarcted rats (n = 5 in each group) were randomly allocated into *1*) vehicle group, *2*) ABT-627, *3*) bosentan, and *4*) hydralazine and were killed at *day 3* after infarction. Hemodynamics and immunohistochemical staining for tyrosine hydroxylase from the remote region were performed at *day 3*. The animal experiment was approved by the Chi-Mei Medical Center and conducted in accordance with its local institutional Guidelines for the Care and Use of Laboratory Animals.

Hemodynamics and infarct size measurements. Hemodynamic parameters were measured in anesthetized rats with ketamine (90 mg/kg ip) at the end of the study (at *day 3* and *week 4*). A polyethylene Millar catheter was inserted into the right carotid artery and connected to a transducer (model SPR-407, Miller Instruments, Houston, TX) to measure LV systolic and diastolic pressure as the mean of measurements of five consecutive pressure cycles as previously described (21). The maximal rate of LV pressure rise (+dP/dt) and decrease (−dP/dt) was measured. After the arterial pressure measurement, the heart was rapidly excised and suspended for retrograde perfusion with a Langendorff apparatus for the electrophysiological tests. At completion of the electrophysiological tests, the atria and the right ventricle were trimmed off, and the LV was rinsed in cold physiological saline, weighed, and immediately frozen in liquid nitrogen after obtaining a coronal section of the LV for infarct size estimation. A section, taken from the equator of the LV, was fixed in 10% formalin and embedded in paraffin for determination of infarct size. Each section was stained with hematoxylin-eosin and trichrome. The infarct size was determined as previously described (21). With respect to clinical importance, only rats with large infarction (>30%) were selected for analysis.

Spontaneous and induced arrhythmias. Each heart was perfused with a modified Tyrode solution containing (in mM) 117.0 NaCl, 23.0 $NaHCO_3$, 4.6 KCl, 0.8 NaH_2PO_4, 1.0 $MgCl_2$, 2.0 $CaCl_2$, and 5.5 glucose, equilibrated at 37°C and oxygenated with a 95% O_2-5% CO_2 gas mixture. The perfusion medium was maintained at a constant temperature of 37°C with a constant flow at 4 ml/min. Epicardial electrograms were recorded by an atraumatic unipolar electrode, placed on the epicardial surface of the right atrium and anterior LV wall 2 mm below the circumflex artery. A bipolar pacing electrode was placed near the apex of the heart on the anterior epicardial surface of the right ventricle. Atrial and ventricular epicardial electrocardiograms were continuously recorded.

After the perfusion of isolated hearts was completed, the hearts were observed for 20 min to allow for a stabilization of contraction and rhythm. Because the residual neural integrity at the infarcted site is one of the determinants of the response to electrical induction of ventricular arrhythmias (15), only rats were included with the infarcted area of the LV totally replaced by scar tissue. The protocol for pacing was modified from that of Nguyen et al. (30). Stimulation intensity was twice the threshold, and stimulus length was 5 ms. The induction of ventricular arrhythmias was then attempted by ventricular stimulation at a basic cycle length of 150 ms (S_0) with single (S_1), double (S_2), and triple (S_3) extrastimuli delivered after eight paced beats. To determine the ventricular effective refractory period (VERP), single extrastimuli was introduced at progressively shorter intervals. VERP was the longest S_1S_2 interval that did not evoke a premature ventricular depolarization. The end point of ventricular pacing was induction of ventricular tachyarrhythmia. A preparation was considered noninducible when pacing produced either no ven-

Table 1. *Cardiac morphology, hemodynamics, and tissue ET-1 concentration at the end of study (week 4)*

	Sham				Infarction with Treatment			
	Vehicle	ABT-627	Bosentan	Hydralazine	Vehicle	ABT-627	Bosentan	Hydralazine
Mortality	0	0	0	0	4	3	4	5
Number of rats	13	13	13	13	13	15	12	13
BW, g	417±7	421±6	425±4	415±5	405±9	418±6	419±6	424±7
Heart rate, beats/min	423±4	419±4	425±6	416±4	424±7	414±5	405±5	427±4
LVESP, mmHg	112±2	88±3‡	90±2‡	92±3‡	99±2*	84±1‡	87±3‡	84±2‡
LVEDP, mmHg	6±1	5±1	5±1	5±1	17±1*	11±1*†	10±1*†	18±1*
+dP/dt, mmHg/s	7,262±145	7,526±126	8,248±154	8,672±157	3,372±84*	4,873±84*†	4,808±129*†	3,128±78*
−dP/dt, mmHg/s	5,423±104	5,636±117	6,712±118	5,772±192	2,346±145*	3,762±148*†	4,523±150*†	3,022±100*
Infarct size, % of LV	—	—	—	—	41±1	40±1	37±1	40±1
LV wt/BW, mg/g	2.15±0.05	2.21±0.04	2.26±0.06	2.24±0.06	2.97±0.08*	2.96±0.08*	2.92±0.09*	3.04±0.11*
RV wt/BW, mg/g	0.58±0.02	0.51±0.01	0.50±0.02	0.52±0.01	0.72±0.04*	0.52±0.02†	0.59±0.01†	0.69±0.03*
Lung wt/BW, mg/g	4.21±0.10	4.15±0.17	4.15±0.12	4.21±0.10	5.44±0.13*	4.49±0.08†	4.62±0.10†	5.64±0.12*
LV ET-1, pg/mg tissue	1.4±0.1	1.3±0.3	1.4±0.1	1.5±0.4	2.5±0.4*	2.9±0.2*	3.1±0.3*	2.7±0.4*

Values are means ± SE. ET-1, endothelin-1; BW, body weight; LVESP, left ventricular (LV) end-systolic pressure; LVEDP, LV end-diastolic pressure; ±dP/dt, maximal rate of LV pressure rise and decrease, respectively; RV, right ventricular. *$P < 0.05$ compared with the respective groups without infarction; †$P < 0.05$ compared with infarcted groups treated with vehicle and hydralazine; ‡$P < 0.05$ compared with the vehicle-treated groups without or with infarction, respectively.

tricular premature contraction or only self-terminating salvos of less than six beats. Ventricular tachyarrhythmias including ventricular tachycardia and ventricular fibrillation were considered nonsustained when it lasted ≤15 beats and sustained when it lasted >15 beats. An arrhythmia scoring system was modified as previously described (30): 0, noninducible preparations; 1, nonsustained tachyarrhythmias induced with three extrastimuli; 2, sustained tachyarrhythmias induced with three extrastimuli; 3, nonsustained tachyarrhythmias induced with two extrastimuli; 4, sustained tachyarrhythmias induced with two extrastimuli; 5, nonsustained tachyarrhythmias induced with one extrastimulus; 6, sustained tachyarrhythmias induced with one extrastimulus; and 7, tachyarrhythmias induced during the eight paced beats. If the heart stopped before the pacing, the arrhythmia score assigned to that heart was 8. When multiple forms of arrhythmias occurred in one heart, the highest score was used. The experimental protocols were typically completed within 10 min. Pilot studies revealed no significant tissue edema during the time period required to complete these experiments.

Real-time RT-PCR of NGF. Real-time quantitative RT-PCR was performed from samples obtained from the remote zone (>2 mm outside the infarct) with the TaqMan system (Prism 7700 Sequence Detection System, PE Biosystems) as previously described (21). For NGF, the primers were 5′-TCCACCCACCCAGTCTTCCA-3′ (sense) and 5′-GCCTTCCTGCTGAGCACACA-3′ (antisense). Coamplification of glyceraldehydes-3-phosphate-dehydrogenase (GAPDH) was used as an internal control in postinfarcted rats as described previously (20). For GAPDH the primers were 5′-CTTCACCACCATGGAGAAGGC-3′ (sense) and 5′-GGCATGGACTGTGGTCATGAG-3′ (antisense). Standard curves were plotted with the threshold cycles versus log template quantities. For quantification, NGF expression was normalized to the expressed housekeeping gene GAPDH. Reaction conditions for 40 cycles of the amplification step were carried out.

Western blot analysis of NGF. Samples obtained from the remote zone were homogenized with a kinametic polytron blender in 100 mM Tris·HCl (pH 7.4), supplemented with 20 mmol/l EDTA, 1 mg/ml pepstatin A, 1 mg/ml antipain, and 1 mmol/l benzamidin. Homogenates were centrifuged at 10,000 *g* for 30 min to pellet the particulate fractions. The supernatant protein concentration was determined with the BCA protein assay reagent kit (Pierce). Twenty micrograms of protein were separated by 10% SDS-PAGE and electrotransferred onto a nitrocellulose membrane. The nitrocellulose membrane was then incubated with rabbit polyclonal anti-NGF antibodies (Chemicon, CA) at 1:1,000 dilution and anti-GAPDH (Cedarline) at 1:1,000 dilution for 2 h. Antigen antibody complexes were detected with horseradish peroxidase substrate (Millipore, Billerica, MA). Films were volume integrated within the linear range of the exposure using a scanning densitometer. Relative abundance was obtained by normalizing the density of NGF protein against that of GAPDH. Experiments were replicated three times, and results were expressed as the mean value.

Immunohistochemical studies of tyrosine hydroxylase, growth-associated protein 43 and neurofilament. To investigate the spatial distribution and quantification of sympathetic nerve fibers, analysis of immunohistochemical staining for tyrosine hydroxylase, growth-associated protein 43 (GAP43; a marker peptide for neuronal regeneration and outgrowth), and neurofilament (a dominant protein of the axonal cytoskeleton; see Ref. 25) was performed on LV muscle from the remote regions. Papillary muscles were excluded from the study because a variable sympathetic innervation has been reported (9). Paraffin-embedded sections were cut at a thickness of 5 μm. Tissues were incubated with anti-tyrosine hydroxylase (1:200; Chemicon), anti-GAP43 (1:400; Chemicon), and antineurofilament (1:1,000; Chemicon, CA) antibodies in 0.5% BSA in PBS overnight at 37°C. Immunostaining was performed using a standard immunoperoxidase technique (N-Histofine Simple Stain MAX PO kit, Nichirei, Tokyo, Japan). Isotype-identical directly conjugated antibodies served as a negative control.

The density of tyrosine hydroxylase-labeled nerve fibers was qualitatively estimated from 10 randomly selected fields at a magnification of ×400. The nerve density was measured on the tracings by computerized planimetry (Image Pro Plus) as described previously (22). The value was expressed as the ratio of tyrosine hydroxylase-labeled nerve fiber area to total area. The slides were coded so that the investigator was blinded to the rat identification.

Laboratory measurements. To examine the sympathetic nerve function after administering ERAs, 20 supplementary infarcted rats ($n = 5$ in each group) were allocated into *1*) vehicle group, *2*) ABT-627 (5 mg·kg^{-1}·day^{-1}), *3*) bosentan (100 mg·kg^{-1}·day^{-1}), and *4*) hydralazine (10 mg·kg^{-1}·day^{-1}). Previous studies have shown the usefulness of the dialysis technique in the in vivo monitoring of regional myocardial interstitial norepinephrine levels (36). Microdialysis probes (13 × 0.2 mm ID; PAN-1200; Asahi Chemical, Tokyo, Japan) with a molecular mass cutoff of 50 kDa were placed in the LV. The dialysis probe was perfused with Ringer solution at a rate of 10 μl/min. One sample period was 4 min. We measured plasma dihydroxyphenylglycol levels (a marker of norepinephrine uptake; see Ref. 11), dialysate norepinephrine levels (a marker of norepinephrine release; see Ref. 36), and LV norepinephrine levels (a marker of norepinephrine store) from remote regions 4 wk after infarction using high-performance liquid chromatography with electrochemical detection (37).

Besides, tissues from the remote zone were obtained for measurements of ET-1 at the end of the study. For ET-1 measurement, the myocardiums were homogenized using a polytron homogenizer for 60 s in 10 vol of 1 mol/l acetic acid containing 10 μg/ml of pepstatin and then immediately boiled for 10 min at 4°C. ET-1 was measured using an immunoassay (R&D Systems, Minneapolis, MN).

Statistical analysis. Results are presented as means ± SE. Statistical analysis was performed using the SPSS statistical package (SPSS, version 10.0, Chicago, IL). Differences among the groups of rats were tested by an ANOVA. Subsequent analysis for significant differences between the two groups was performed with a multiple comparison test (Scheffé's method). Electrophysiological data (scoring of programmed electrical stimulation-induced arrhythmias) were compared by a Kruskal-Wallis test, followed by a Mann-Whitney test. The significant level was assumed at a value of $P < 0.05$.

RESULTS

We found no significant differences in mortality among the infarcted groups throughout the study (Table 1). Either selective ET_A or nonselective ET_A/ET_B blockade had little effect on cardiac gross morphology in the sham-operated rats. Four weeks after infarction, the infarcted area of the LV was very

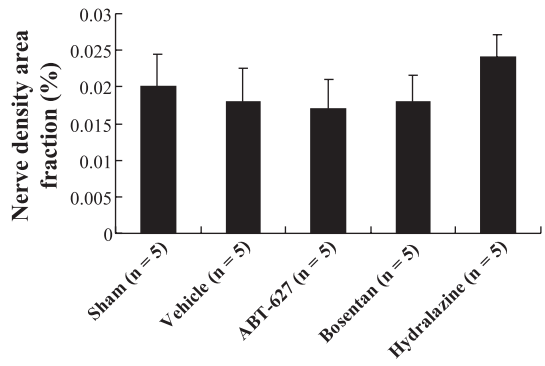

Fig. 1. At *postinfarction day 3*, quantitative analysis of immunohistochemical staining for tyrosine hydroxylase from the remote regions. There were similar nerve densities among the infarcted groups. *n*, Number of rats.

thin and was totally replaced by fully differentiated scar tissue. The weight of the LV inclusive of the septum remained essentially constant 4 wk after coronary artery occlusion among the infarcted groups. Infarct size did not differ among the infarcted groups.

Hemodynamics. After 4 wk of treatment in infarcted rats, ET_A blockade and combined ET_A/ET_B blockade decreased systolic blood pressure significantly and to a similar extent (Table 1). Chronic treatment with hydralazine led to a similarly lower systolic blood pressure compared with ERAs-treated infarcted rats. There was no significant difference of blood pressure in infarcted rats with the same treatment between *day 3* and *week 4* (data not shown). $+dP/dt$ and $-dP/dt$ were significantly improved in the ERAs-treated infarcted groups

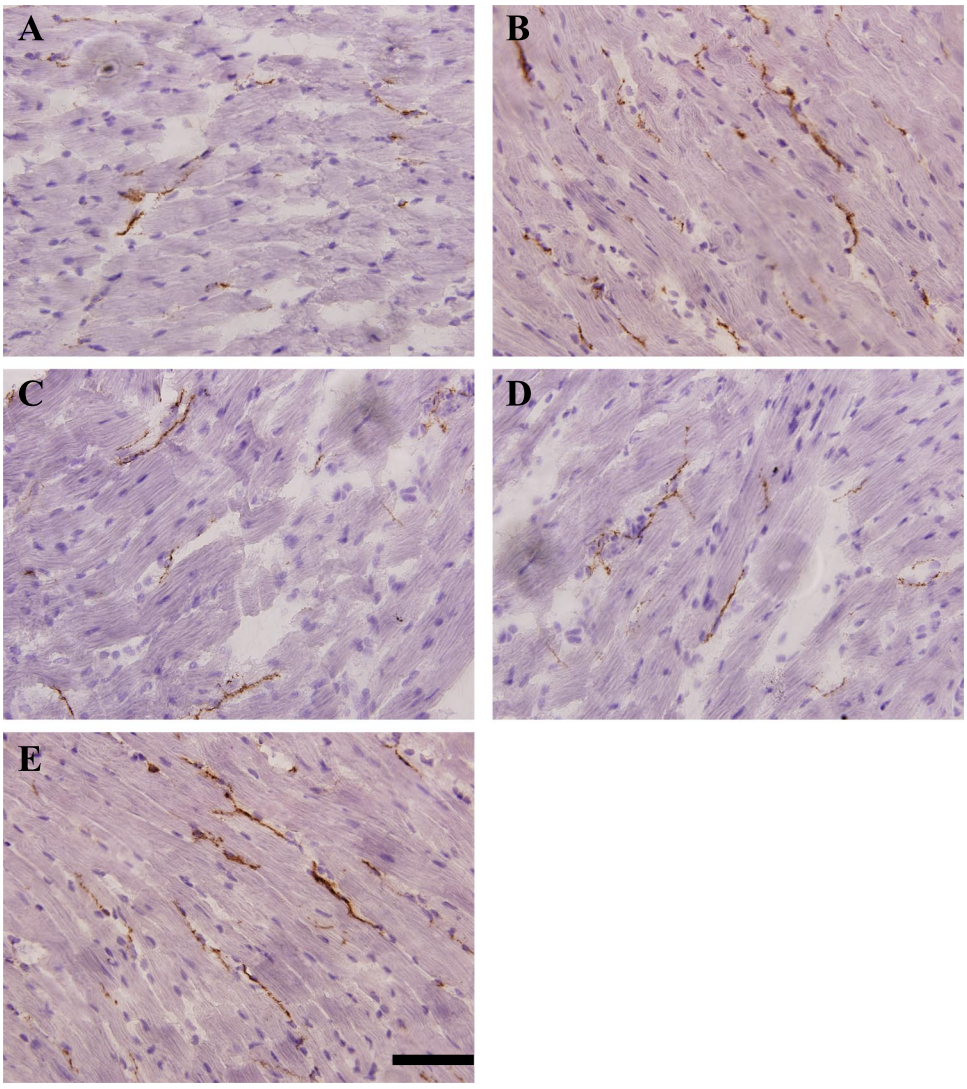

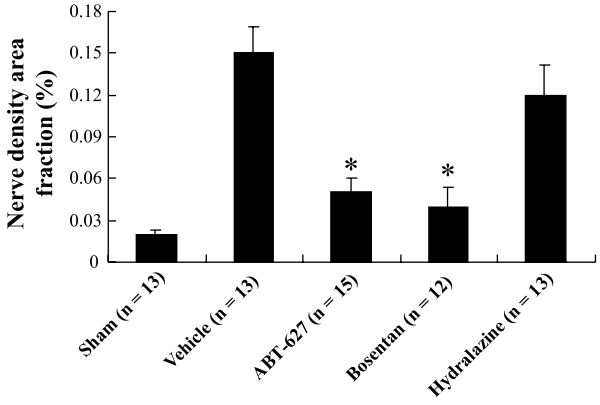

Fig. 2. *Top*: at *postinfarction week 4*, immunohistochemical staining for tyrosine hydroxylase from the remote regions (magnification, ×400). Tyrosine hydroxylase-positive nerve fibers (brown color) are located between myofibrils and are oriented longitudinal direction as that of the myofibrils. Myocytes are not stained and appear pale in this view. Sham (*A*), vehicle (*B*), ABT-627 (*C*), bosentan (*D*), and hydralazine (*E*) are shown. Bar = 50 μm. *Bottom*: nerve density area fraction (in %) at the remote zone. *$P <$ 0.05 compared with vehicle- and hydralazine-treated groups.

compared with infarcted groups treated with vehicle or hydralazine.

Myocardial ET-1 levels. When compared with sham-operated animals, tissue levels of ET-1 from the remote regions were significantly increased in infarcted vehicle-treated infarcted animals (1.4 ± 0.1 vs. 2.5 ± 0.4 pg/mg tissue in infarcted rats; $P < 0.05$, Table 1). When compared with the infarcted group treated with vehicle, neither an ET_A nor a combined ET_A/ET_B blocker affected the levels of tissue ET-1 (2.9 ± 0.2 and 3.1 ± 0.3 pg/mg tissue, respectively).

Immunohistochemical analyses. The tyrosine hydroxylase-immunostained nerve fibers appeared to be oriented in the longitudinal axis of adjacent myofibers. At *day 3*, there was no significant quantitative difference of tyrosine hydroxylase-positive nerve area fraction among the infarcted groups (Fig. 1). At *week 4*, the tyrosine hydroxylase-positive nerve area fraction was significantly larger in vehicle-treated infarcted rats than that in the sham-operated group (Fig. 2). At *week 4*, the tyrosine hydroxylase-positive nerve area fraction was not significantly different in the sham-operated groups treated with vehicle, ABT-627, or bosentan (data not shown). Infarcted rats in the ABT-627- and bosentan-treated groups showed smaller nerve area fractions in the remote regions than rats in the vehicle-treated infarcted group (0.05 ± 0.01% and 0.04 ± 0.01% vs. 0.15 ± 0.02% in vehicle group, $P < 0.001$, respectively). Similar to tyrosine hydroxylase results, GAP43- (Fig. 3) and neurofilament-positive (data not shown) nerve area fractions were significantly attenuated in the ABT-627- and bosentan-treated infarcted rats compared with vehicle-treated infarcted rats. The rats given hydralazine developed significantly stronger immunostained profiles than rats given ERAs (Fig. 2).

Western blot analyses and real-time PCR of NGF. Western blot analysis shows that NGF levels are significantly upregulated 4.9-fold at the remote zone in the vehicle-treated infarcted rats than in the sham-operated rats ($P < 0.0001$, Fig. 4). When compared with vehicle-treated infarcted rats in ABT-627- and bosentan-treated rats, NGF levels were significantly lower at the remote zone. The protein expression level of NGF was similar in the hydralazine-treated group compared with that in the vehicle-treated infarcted rats.

PCR amplification of the cDNA revealed that the NGF mRNA levels showed a 1.9-fold upregulation at the remote zone in the vehicle compared with the sham-operated rats ($P < 0.0001$, Fig. 5). In either ABT-627- or bosentan-treated in-

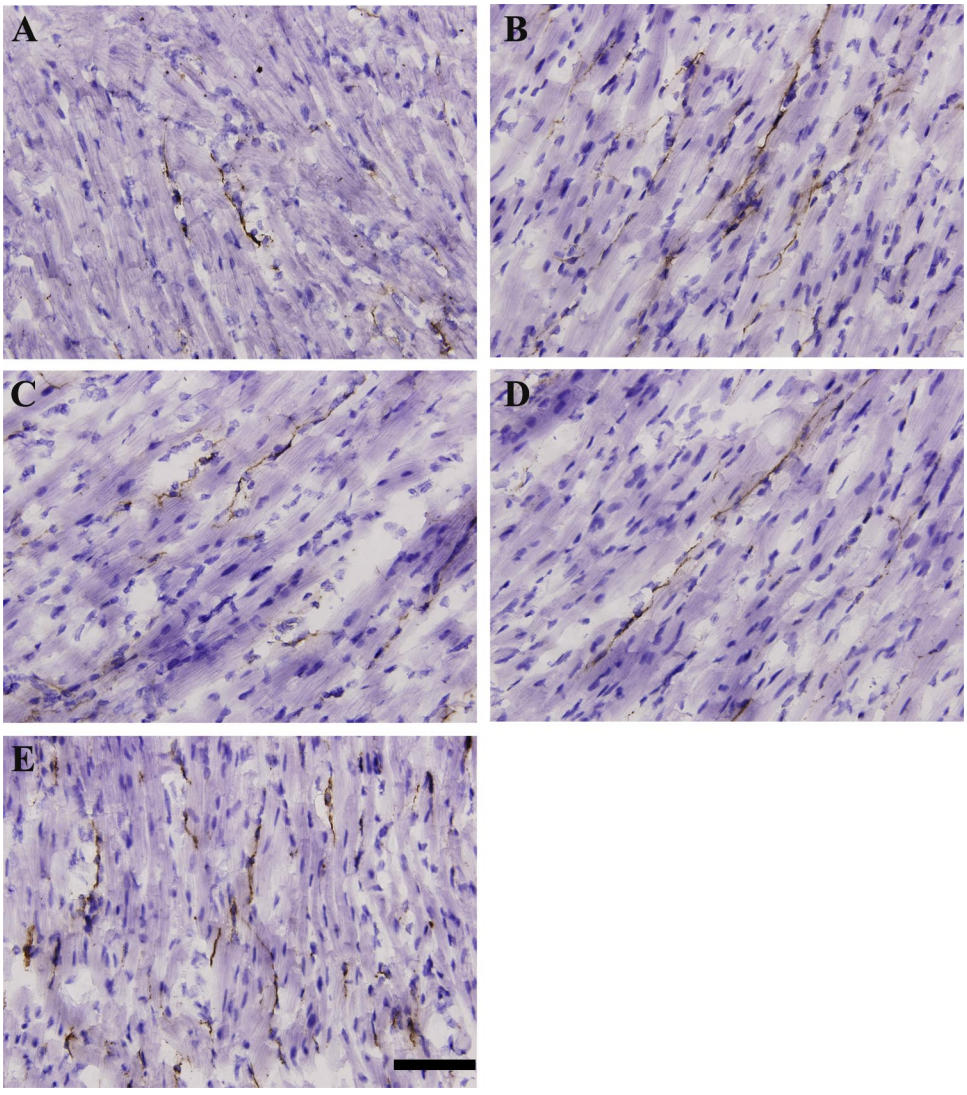

Fig. 3. Immunohistochemical staining for growth-associated protein 43 (GAP43) from the remote regions (magnification, ×400). GAP43-positive staining was markedly increased in infarcted groups treated with vehicle and hydralazine. Sham (*A*), vehicle (*B*), ABT-627 (*C*), bosentan (*D*), and hydralazine (*E*) are shown. Bar = 50 μm.

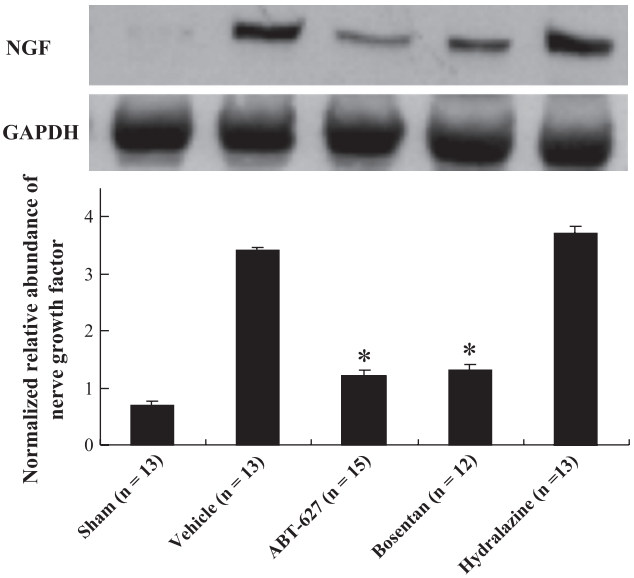

Fig. 4. Western blot analysis of nerve growth factor (NGF; molecular mass, 13 kDa) in homogenates of the left ventricle (LV) from the remote zone. Quantitative analysis results for NGF obtained by densitometry from the same blots. When compared with vehicle-treated infarcted rats in ABT-627- and bosentan-treated rats, NGF levels were significantly lower. Relative abundance was obtained by normalizing the density of NGF protein against that of GAPDH. Results are means ± SE of 3 independent experiments. *$P < 0.05$ compared with vehicle- and hydralazine-treated groups.

farcted rats, the NGF mRNA levels were significantly decreased compared with those in the vehicle. The attenuated magnitude of NGF mRNA levels was similar between ABT-627- and bosentan-treated rats. NGF protein expression was in parallel to the mRNA level changes, implying that the NGF production is a critical regulation step for nerve sprouting.

Electrophysiological stimulation. To further elucidate the physiological effect of attenuated sympathetic reinnervation, ventricular pacing was performed. Neither ERAs nor hydralazine had any statistically significant effect on VERP in the sham-operated groups. In the vehicle-treated infarcted group, VERP was significantly reduced by 19 ± 2 ms compared with sham-operated rats treated with vehicle ($P < 0.001$, Fig. 6). ABT-627 and bosentan treatment significantly reduced the

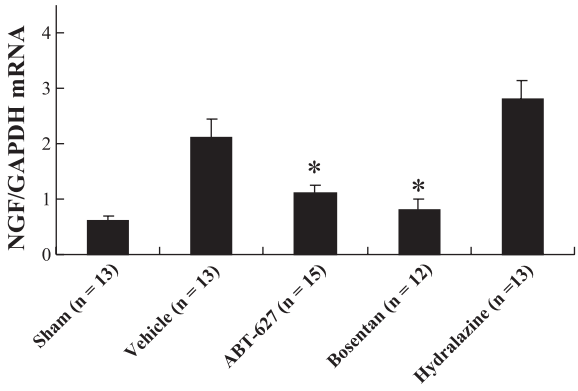

Fig. 5. LV NGF mRNA levels. Each mRNA was corrected for an mRNA level of GAPDH. Each column and bar represent means ± SE. *$P < 0.05$ compared with vehicle- and hydralazine-treated groups.

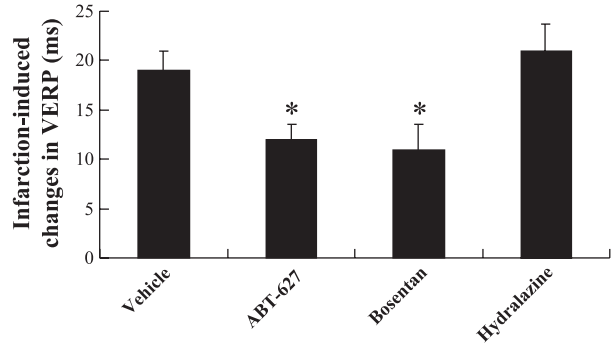

Fig. 6. Infarction significantly reduced ventricular effective refractory period (VERP). Either ABT-627 or bosentan administration significantly attenuated the shortening of VERP compared with vehicle-treated infarcted rats. *$P < 0.05$ compared with vehicle- and hydralazine-treated groups.

infarction-induced shortening of VERP by 37% and 42% ($P = 0.006$ and <0.001), respectively.

A representative electrocardiogram record in a vehicle-treated infarcted rat is shown in Fig. 7. Arrhythmia score in sham-operated rats was very low (0.2 ± 0.1; Fig. 8). In contrast, ventricular tachyarrhythmias consisting of ventricular tachycardia and ventricular fibrillation were inducible by programmed stimulation in vehicle-treated infarcted rats. ABT-627 and bosentan treatment significantly decreased the inducibility of ventricular tachyarrhythmias compared with vehicle and hydralazine treatment.

Sympathetic nerve function. Plasma dihydroxyphenylglycol levels were significantly upregulated 3.3-fold at the remote zone in the vehicle-treated infarcted rats than in sham-operated rats (5,472 ± 142 vs. 1,682 ± 113 pg/ml, $P < 0.001$, Fig. 9). When compared with vehicle-treated infarcted rats, plasma dihydroxyphenylglycol levels were significantly lower at the remote zone in ABT-627- and bosentan-treated rats. Dialysate norepinephrine levels and LV norepinephrine levels showed similar changes to plasma dihydroxyphenylglycol levels.

DISCUSSION

Our present study shows for the first time that chronic treatment for 4 wk with ERAs leads to attenuated sympathetic

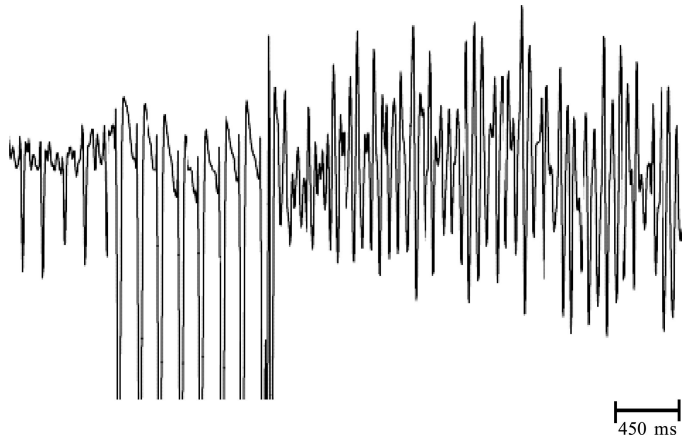

Fig. 7. A representative sustained ventricular arrhythmias induced by ventricular pacing in an infarcted rat treated with vehicle. Following 8 basic stimuli at a cycle length of 150 ms, 2 extra stimuli were applied at progressively shorter coupling intervals (score: 4).

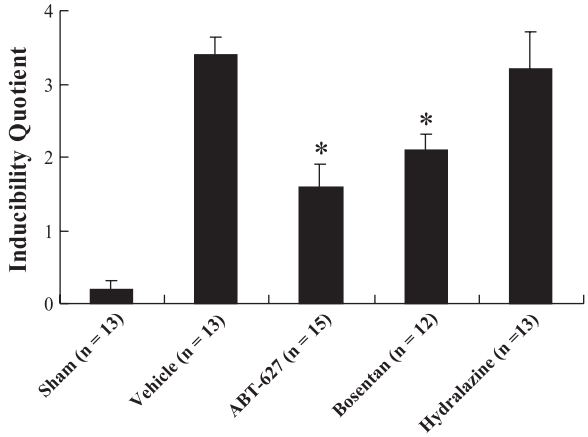

Fig. 8. Inducibility quotient of ventricular arrhythmias by programmed electrical stimulation 4 wk after myocardial infarction. *$P < 0.05$ compared with infarcted groups treated with vehicle- and hydralazine-treated groups.

reinnervation after myocardial infarction. These results were concordant with beneficial effects of ERAs, as documented structurally by a reduction in cardiac nerve sprouting, molecularly, by myocardial NGF protein and mRNA levels, biochemically, by tissue ET-1 levels and sympathetic nerve function, and electrophysiologically, by reduced extent of infarction-induced VERP shortening and improvement of fatal ventricular tachyarrhythmias. The beneficial effects of ERAs as antiarrhythmic agents may be related to the remodeling of the sympathetic nervous system that is mediated by the ET-1/NGF pathway.

The beneficial effect of ERAs on sympathetic reinnervation was supported by three lines of evidence. First, excessive sympathetic reinnervation was observed at the remote zone at *week 4* but not at *day 3*. The finding was compatible with the notion that an infarcted myocardium causes a disappearance of sympathetic innervation which is followed by a phase of excessive sympathetic reinnervation (13). Since the morphological features of sympathetic reinnervation were increased at 4 wk after infarction, sympathetic nerve function assessed by the norepinephrine content of myocardium and the dialysate and plasma dihydroxyphenylglycol levels showed significant increase. Thus the structural features of sympathetic ingrowth are established not only at anatomical impact but also at functional features of this sprouting phenomenon. Second, the current results confirmed our previous study that the ET-1 level was significantly increased after infarction (21). The chronic blockade of nonselective ET_A/ET_B receptors attenuated sympathetic reinnervation at the remote zone, to the same extent as ET_A receptor blockade alone. Although we did not use selective ET_B receptor antagonists, a similar potency to attenuate reinnervation by ABT-627 and bosentan may suggest that ET_A, but not ET_B, plays a role in mediating sympathetic reinnervation. However, the present results have not totally dismissed a role of ET_B in sympathetic reinnervation. Although dissimilar structures, both ERAs appear to share a common mediator, NGF, in which transcription and translation levels of NGF may play a role in the signal transduction pathway. Furthermore, there was similar sympathetic attenuation at *day 3* among the infarcted groups, implying that ERAs inhibited sympathetic reinnervation at the late stage of infarction and not enhanced nerve degeneration at the early stage of infarction. Third, the severity of pacing-induced fatal arrhythmias was associated with the degree of sympathetic reinnervation. The finding was further supported by Cao et al. (6, 7), showing that increased postinjury sympathetic nerve density may be responsible for the occurrence of ventricular arrhythmia and sudden cardiac death in animals and patients.

Mechanisms. In this study, we demonstrated attenuated sympathetic reinnervation in ERA-treated hearts. The detailed mechanisms by which ERAs affect sympathetic reinnervation remain undefined. However, several factors can be excluded. First, there are hemodynamics. Although both ERAs effectively lowered blood pressure, the mechanism by which ERAs prevent sympathetic reinnervation is probably not due to its antihypertensive effect alone. Because of the lack of effect of hydralazine on attenuating sympathetic reinnervation, it would

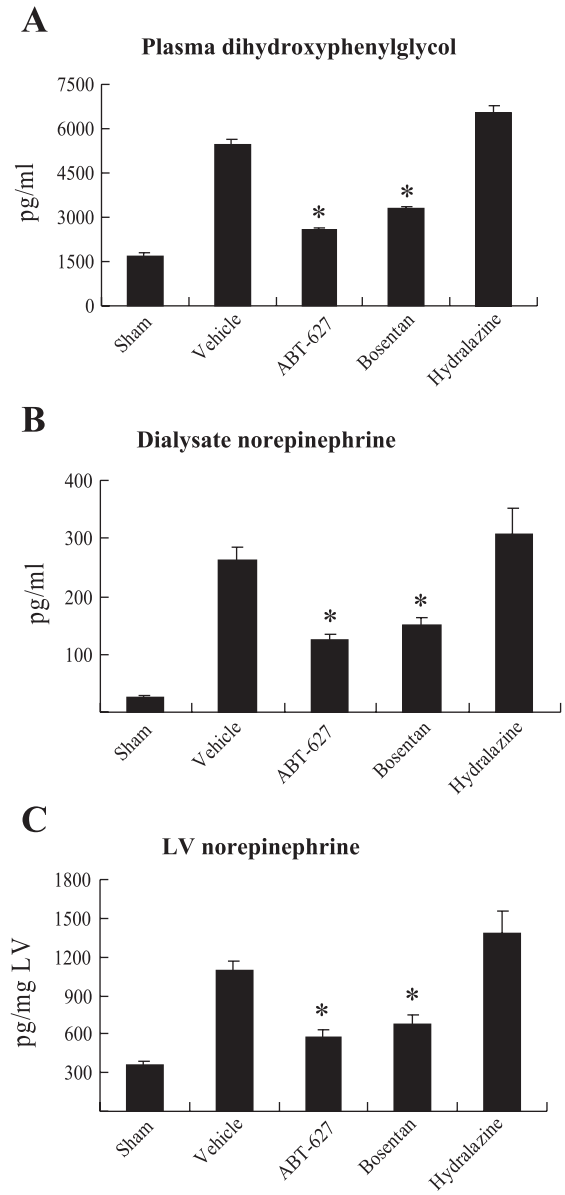

Fig. 9. Effect of endothelin receptor antagonists on plasma dihydroxyphenylglycol levels (*A*), dialysate norepinephrine levels (*B*), and LV norepinephrine levels (*C*) 4 wk after infarction ($n = 5$ in each group). Results are given as means ± SE. *$P < 0.05$ compared with vehicle group.

appear that arterial pressure is not enough to prevent ongoing sympathetic reinnervation. Some factors other than blood pressure may contribute to the pathogenesis of excessive sympathetic reinnervation after infarction. Second, there are differences in infarct sizes. The degree of sympathetic reinnervation has been related to the infarct sizes (12). Successful fiber reinnervation appears dependent on repopulating sheaths with Schwann cells, which would be injured according to the size of infarction. This possibility was excluded in this study due to similar infarct sizes among the infarcted groups.

Our results showed that attenuated sympathetic reinnervation after ERA administration has benefits not only in anatomical structures but also in arrhythmia susceptibility. The ET receptor subtypes are distributed differently within the heart: ET_A receptors are localized primarily on myocytes and cells of the conduction system, whereas ET_B receptors are found primarily on endothelium (26). This specific distribution pattern explained, at least in part, our results, showing that the effects of chronic selective ET_A blockade on cardiac electrical activity were quantitatively similar to those induced by combined ET_A/ET_B blockade. Furthermore, the NGF promoter contains both activator protein-1 and CCAAT/enhancer-binding protein d elements (8). ET-1 significantly augmented luciferase activity from the full-length NGF promoter, but deletion of the activator protein-1 element markedly decreased this augmentation (17). The truncation plasmids revealed that the CCAAT/enhancer-binding protein d element was also involved in this induction of NGF. In fact, ET-1-induced NGF augmentation was mediated by the ET_A receptor, Gi$\beta\gamma$, PKC, the Src family, EGFR, extracellular signal-regulated kinase, p38MAPK, activator protein-1, and the CCAAT/enhancer-binding protein d element (17). The notion was consistent with out results that ERAs, especially for ET_A antagonists, in the reinnervated regions caused greater reduction in regional expression of NGF at the transcription levels.

Other mechanisms. Although the present study suggests that the mechanisms of ERA-induced neuroprotection are related to attenuated NGF expression, other potential mechanisms need to be studied, such as electrical remodeling and cardiac fibrosis. First, the ET_A receptor antagonist might prevent fatal arrhythmias by directly inhibiting electrophysiological alterations (24). ET-1 directly inhibited the potassium channel and was an important mediator of arrhythmogenesis (18). Long-term treatment with an ET_A receptor antagonist prevented electrical remodeling, such as reducing transient outward current, delayed rectifier potassium current, and L-type calcium current, and prolonged action potential duration in ventricular cells in cardiomyopathic hamsters (24). All of the above ion channels are important for the induction of abnormal automaticity and reentrant arrhythmias. Preventing ionic remodeling may be an upstream approach to antiarrhythmic therapy (29). Second, ET_A antagonist prevented cardiac fibrosis (2), thereby reducing the risk of isolated regional slowing of conduction and reentrant arrhythmias.

Study limitations. There are some limitations in the present study that have to be acknowledged. Our finding in rats cannot necessarily be extrapolated to humans with myocardial infarction. Different species have been shown to have a different distribution of ET receptor population. The contribution of ET_A receptors has been shown to assume a lesser significance in humans because they account for up to 60% of the total ET receptors in ventricular myocardium compared with 85% in rat ventricular myocardium (27).

Conclusions. These data show that the ET system, especially via ET_A receptors, plays an important role in the sympathetic reinnervation after infarction. These effects are functionally and structurally important because they are linked to attenuated incidence of fatal arrhythmias. Either ET_A or ET_A/ET_B blockade may provide a new strategy for the prevention of postinfarction ventricular arrhythmias. Further studies of the specific role of ERAs in the myocardium may contribute to our understanding of their neuroprotective actions and to the development of novel neuroprotective therapies.

ACKNOWLEDGMENTS

We thank Chung-San Huang, Yu-Wei Chao, and Shen-Chuan Chen for their excellent technical assistance. ABT-627 was a generous gift from the Abbott Park, IL. Bosentan was a generous gift from the Actelion Pharmaceuticals Ltd. Allschwil, Switzerland.

GRANTS

This work was supported by Chi-Mei Medical Center Grants CMFHT9501, CMFHR9502, CMFHR9506, and CM-TMU9601 and the National Science Council, Republic of China, Grants NSC-96-2314-B-384-008.

REFERENCES

1. **Alexander BT, Rinewalt AN, Cockrell KL, Massey MB, Bennett WA, Granger JP.** Endothelin type a receptor blockade attenuates the hypertension in response to chronic reductions in uterine perfusion pressure. *Hypertension* 37: 485–489, 2001.
2. **Ammarguellat F, Larouche I, Schiffrin EL.** Myocardial fibrosis in DOCA-salt hypertensive rats: effect of endothelin ET_A receptor antagonism. *Circulation* 103: 319–324, 2001.
3. **Bélichard P, Savard P, Cardinal R, Nadeau R, Gosselin H, Paradis P, Rouleau JL.** Markedly different effects on ventricular remodeling result in a decrease in inducibility of ventricular arrhythmias. *J Am Coll Cardiol* 23: 505–513, 1994.
4. **Brauer MM, Chavez-Genaro R, Llodra J, Richeri A, Scorza MC.** Effects of chronic oestrogen treatment are not selectively for uterine noradrenaline-containing sympathetic nerves: a transplantation study. *J Anat* 196: 347–355, 2000.
5. **Brennan C, Rivas-Plata K, Landis SC.** The p75 neurotrophin receptor influences NT-3 responsiveness of sympathetic neurons in vivo. *Nat Neurosci* 2: 699–705, 1999.
6. **Cao JM, Chen LS, KenKnight BH, Ohara T, Lee MH, Tsai J, Lai WW, Karagueuzian HS, Wolf PL, Fishbein MC, Chen PS.** Nerve sprouting and sudden cardiac death. *Circ Res* 96: 816–821, 2000.
7. **Cao JM, Fishbein MC, Han JB, Lai WW, Lai AC, Wu TJ, Czer L, Wolf PL, Denton TA, Shintaku IP, Chen PS, Chen LS.** Relationship between regional cardiac hyperinnervation and ventricular arrhythmias. *Circulation* 101: 1960–1969, 2000.
8. **Colangelo AM, Johnson PF, Mocchetti I.** Beta-adrenergic receptor-induced activation of nerve growth factor gene transcription in rat cerebral cortex involves CCAAT/enhancer-binding protein delta. *Proc Natl Acad Sci USA* 95: 10920–10925, 1998.
9. **Dahlstrom A.** Observations on the accumulation of noradrenaline in the proximal and distal parts of peripheral adrenergic nerves after compression. *J Anat* 99: 677–689, 1965.
10. **Du XJ, Cox HS, Dart AM, Esler MD.** Sympathetic activation triggers ventricular arrhythmias in rat heart with chronic infarction and failure. *Cardiovasc Res* 43: 919–929, 1999.
11. **Goldstein DS, Eisenhofer G, Stull R, Folio CJ, Keiser HR, Kopin IJ.** Plasma dihydroxyphenylglycol and the intraneuronal disposition of norepinephrine in humans. *J Clin Invest* 81: 213–220, 1988.
12. **Gulati AK.** Evaluation of acellular, and cellular nerve grafts in repair of rat peripheral nerve. *J Neurosurg* 68: 117–123, 1988.
13. **Hasan W, Jama A, Donohue T, Wernli G, Onyszchuk G, Al-Hafez B, Bilgen M, Smith PG.** Sympathetic hyperinnervation and inflammatory cell NGF synthesis following myocardial infarction in rats. *Brain Res* 1124: 142–154, 2006.

14. **Hassankhani A, Steinhelper ME, Soonpaa MH, Katz EB, Taylor DA, Andrade-Rozental A, Factor SM, Steinberg JJ, Field LJ, Federoff HJ.** Overexpression of NGF within the heart of transgenic mice causes hyperinnervation, cardiac enlargement, and hyperplasia of ectopic cells. *Dev Biol* 169: 309–321, 1995.
15. **Herre JM, Wetstein L, Lin YL, Mills AS, Dae M, Thames MD.** Effect of transmural versus nontransmural myocardial infarction on inducibility of ventricular arrhythmias during sympathetic stimulation in dogs. *J Am Coll Cardiol* 11: 414–421, 1988.
16. **Heumann R, Korsching S, Scott J, Thoenen H.** Relationship between levels of nerve growth factor (NGF) and its messenger RNA in sympathetic ganglia and peripheral target tissues. *EMBO J* 3: 3183–3189, 1984.
17. **Ieda M, Fukuda K, Hisaka Y, Kimura K, Kawaguchi H, Fujita J, Shimoda K, Takeshita E, Okano H, Kurihara Y, Kurihara H, Ishida J, Fukamizu A, Federoff HJ, Ogawa S.** Endothelin-1 regulates cardiac sympathetic innervation in the rodent heart by controlling nerve growth factor expression. *J Clin Invest* 113: 876–884, 2004.
18. **James AF, Ramsey JE, Reynolds AM, Hendry BM, Shattock MJ.** Effects of endothelin-1 on K^+ current from rat ventricular myocytes. *Biochem Biophys Res Commun* 284: 1048–1055, 2001.
19. **Lai AC, Wallner K, Cao JM, Chen LS, Karagueuzian HS, Fishbein MC, Chen PS, Sharifi BG.** Colocalization of tenascin and sympathetic nerves in a canine model of nerve spouting and sudden cardiac death. *J Cardiovasc Electrophysiol* 11: 1345–1351, 2000.
20. **Lax CJ, Domenighetti AA, Pavia JM, Di Nicolantonio R, Curl CL, Morris MJ, Delbridge LM.** Transitory reduction in angiotensin AT_2 receptor expression levels in postinfarct remodelling in rat myocardium. *Clin Exp Pharmacol Physiol* 31: 512–517, 2004.
21. **Lee TM, Chou TF, Tsai CH.** Effects of pravastatin on cardiomyocyte hypertrophy and ventricular vulnerability in normolipidemic rats after myocardial infarction. *J Mol Cell Cardiol* 35: 1449–1459, 2003.
22. **Lee TM, Lin MS, Chou TF, Tsai CH, Chang NC.** Adjunctive 17β-estradiol administration reduces infarct size by altered expression of canine myocardial connexin43 protein. *Cardiovasc Res* 63: 109–117, 2004.
23. **Lockhart ST, Turrigiano GG, Birren SJ.** Nerve growth factor modulates synaptic transmission between sympathetic neurons and cardiac myocytes. *J Neurosci* 17: 9573–9582, 1997.
24. **Matsumoto Y, Aihara H, Yamauchi-Kohno R, Reien Y, Ogura T, Yabana H, Masuda Y, Sato T, Komuro I, Nakaya H.** Long-term endothelin A receptor blockade inhibits electrical remodeling in cardiomyopathic hamsters. *Circulation* 106: 613–619, 2002.
25. **Meiri KF, Pfenninger KH, Willard MB.** Growth-associated protein, GAP-43, a polypeptide that is induced when neurons extend axons, is a component of growth cones and corresponds to pp46, a major polypeptide of a subcellular fraction enriched in growth cones. *Proc Natl Acad Sci USA* 83: 3537–3541, 1986.
26. **Modesti PA, Vanni S, Paniccia R, Bandinelli B, Bertolozzi I, Polidori G, Sani G, Neri Serneri GG.** Characterization of endothelin-1 receptor subtypes in isolated human cardiomyocytes. *J Cardiovasc Pharmacol* 34: 333–339, 1999.
27. **Molenaar P, O'Reilly G, Sharkey A.** Characteristics and localisation of endothelin receptor subtypes in the human AV conducting system and myocardium. *Circ Res* 72: 526–538, 1993.
28. **Mulder P, Richard V, Derumeaux G, Hogie M, Henry JP, Lallemand F, Compagnon P, Macé B, Comoy E, Letac B, Thuillez C.** Role of endogenous endothelin in chronic heart failure: effect of long-term treatment with an endothelin antagonist on survival, hemodynamics, and cardiac remodeling. *Circulation* 96: 1976–1982, 1997.
29. **Nattel S, Li D.** Ionic remodeling in the heart: pathophysiological significance and new therapeutic opportunities for atrial fibrillation. *Circ Res* 87: 440–447, 2000.
30. **Nguyen T, El Salibi E, Rouleau JL.** Postinfarction survival and inducibility of ventricular arrhythmias in the spontaneously hypertensive rat: effects of ramipril and hydralazine. *Circulation* 98: 2074–2080, 1998.
31. **Rich S, McLaughlin VV.** Endothelin receptor blockers in cardiovascular disease. *Circulation* 108: 2184–2190, 2003.
32. **Sakai S, Miyauchi T, Yamaguchi I.** Long-term endothelin receptor antagonist administration improves alterations in expression of various cardiac genes in failing myocardium of rats with heart failure. *Circulation* 101: 2849–2853, 2000.
33. **Snider WD.** Functions of the neurotrophins during nervous system development: what the knockouts are teaching us. *Cell* 77: 627–638, 1994.
34. **Vracko R, Thorning D, Frederickson RG.** Fate of nerve fibers in necrotic, healing, and healed rat myocardium. *Lab Invest* 63: 490–501, 1990.
35. **Xia QG, Chung O, Spitznagel H, Illner S, Jänichen G, Rossius B, Gohlke P, Unger T.** Significance of timing of angiotensin AT_1 receptor blockade in rats with myocardial infarction-induced heart failure. *Cardiovasc Res* 49: 110–117, 2001.
36. **Yamazaki T, Akiyama T, Kitagawa H, Takauchi Y, Kawada T, Sunagawa K.** A new, concise dialysis approach to assessment of cardiac sympathetic nerve terminal abnormalities. *Am J Physiol Heart Circ Physiol* 273: H1182–H1187, 1997.
37. **Yamazaki T, Akiyama T, Shindo T.** Routine high-performance liquid chromatographic determination of myocardial interstitial norepinephrine. *J Chromatogr B Biomed Appl* 670: 328–331, 1995.